New Journal of Physics
The open access journal at the forefront of physics

Deutsche Physikalische Gesellschaft DPG
IOP Institute of Physics

Published in partnership with: Deutsche Physikalische Gesellschaft and the Institute of Physics

PAPER

Communicability geometry of multiplexes

Ernesto Estrada

Institute of Applied Mathematics (IUMA), Universidad de Zaragoza, Pedro Cerbuna 12, E-50009 Zaragoza, Spain
ARAID Foundation, Government of Aragón, E-50018 Zaragoza, Spain

E-mail: ernesto.estrada.roger@gmail.com

Keywords: multiplex networks, communicability, diffusion, matrix functions, Euclidean geometry

OPEN ACCESS

RECEIVED
12 October 2018

REVISED
12 December 2018

ACCEPTED FOR PUBLICATION
14 December 2018

PUBLISHED
25 January 2019

Abstract

We give a formal definition of a multiplex network and using its supra-adjacency matrix representation we construct the multiplex communicability matrix. Then we prove that the communicability function naturally induces an embedding of the multiplexes in a hyperspherical Euclidean space. We then study (i) intra-layer, (ii) inter-layer, and (iii) inter-layer self-communicability distance and angles in multiplex networks. Using these multiplex metrics we study a social multiplex related to an office politics and the multiplex of synaptic interactions between neurons in the worm *C. elegans*. We find that the average communicability angles in these multiplexes exhibits a minimum for certain value of the interlayer coupling strength. We provide an explanation for this phenomenon which emerges from the multiplexity of these systems and related it to other important phenomena like the synchronizability of these systems. Finally, we define and study communicability shortest paths in the multiplexes. We show how the communicability shortest paths avoid the most central nodes in the multiplexes in terms of their degree and betweenness, which is a main difference with (topological) shortest paths. We explain this behavior in terms of a diffusive model in which the 'information' not only diffuses between the nodes but it is also processed internally on the entities of the complex system. Finally, we give some new ideas on how to extend the current work and represent complex systems as 'multiplex hypergraphs' and 'multi-simplicial complexes'.

1. Introduction

A characteristic feature of complex systems is that they are composed by individual entities that interact with each other in some way [1–4]. Capturing these connectivity patterns is not a trivial task as it depends on the type of interaction considered and the level of detail in which such interactions are studied. Let us consider the paradigmatic case of social interactions. We can consider a group of individuals which interchange information among them. The first approach consists in observing who shares information to whom and constructing a set of binary relations that can be easily represented by a graph $G = (V, E)$ where the set of nodes represents the individuals and the set of edges their pairwise interactions. We can then extend our representation by considering the frequency of interactions between the individuals and then creating a weighted graph $G = (V, E, \mathcal{F}, \varrho)$ where ϱ: $\mathcal{F} \rightarrow E$ is a surjective mapping assigning frequencies of interaction (weights) to edges [5, 6]. As part of the natural evolution of the social group we can also observe that individuals form groups and that now the interactions are between groups more than pairwise. Thus, the system should now be represented as a hypergraph $H = (V, \mathscr{E})$ where the set of hyperedges $\mathscr{E}$ accounts for any k-ary relation between the agents in the system [7–9]. Obviously, this hypergraph can also be directed and weighted with the corresponding adaptations of the representation system used [10, 11]. In the hypergraph representation we consider that every group (hyperedge) act as a unit of the system and subsets of them do not form subunits of the global system. This is the case for instance where four people in one of the groups have a chat in which everybody can listen to each other [12]. Mathematically, this situation is represented by the fact that this set of individuals is closed under the subset operation, meaning that all subsets (triangles and edges) inside the corresponding set (tetrahedron) are also members of the system [12–17]. In this case the conversation is not pairwise as represented

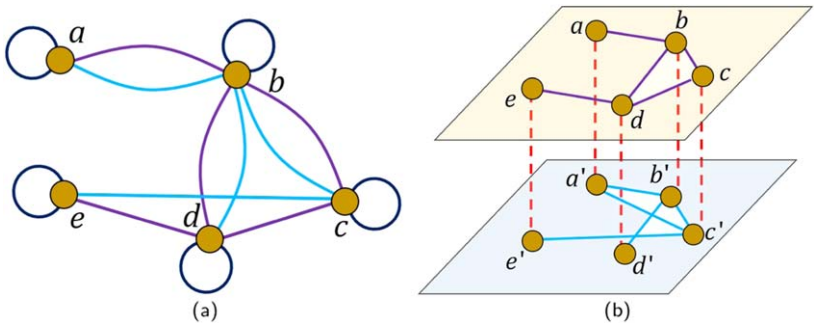

Figure 1. Representation of a complex system as a colored pseudo-multigraph (a) and as a multiplex.

by the graph, and is not even in the form of the hyper-edge represented by the hypergraph, but a combination of the tetrahedrons, triangles and edges. Thus, a simplicial complex is defined by $\mathcal{K} = (V, \Sigma)$ where Σ is a set of simplices, such that every face from $\mathcal{K}$ is also in $\mathcal{K}$, and the intersection of any two simplices is a face of both simplices [12–17].

Even at this level of sophistication in which we dispose of graphs, hypergraphs and simplicial complexes, there are important aspects of complex systems not captured by these representations. Returning to the example of social interactions we can consider that the same group of agents are interacting by different channels, such as face-to-face, Facebook, Twitter, etc. A way of representing this complex scenario is through the use of colored multigraphs, particularly using the concept of properly colored walks [18]. This complicated representation consists of the set of vertices, a set of edges, a mapping assigning edges to pairs of nodes (to allow multiple edges), a set of weighted self-loops controlling the hopping between layers, a set of colors, and another mapping assigning colors to edges and self-loops. For instance, if a group of five people interact face-to-face and via Twitter we need three colors, one for the face-to-face interaction, one for the Twitter interaction and another for the self-loops connecting the two colors. This is illustrated in figure 1(a). A more appealing pictorial representation of this interaction scenario is by slicing the nodes into different layers, one per type of interactions, forming a multiplex [19–21]. Instead of the self-loops we now have edges connecting the nodes in one layer to themselves in another layer, and the edges with the same color are all in the same layer. This is represented in figure 1(b). Although both representations are equivalent, there are areas in which the multiplex representation is more convenient. Currently, there is a vast literature about the use of multiplexes for representing complex systems, mainly about the characterization of their structural properties [22–24] and the associated critical phenomena [25–30], where it has been shown for instance that multiplexes display a transition from a regime in which the system behaves as a set of independent networks to the one in which a coordinated behavior emerges [31, 32].

Here we start by giving a formal definition of a multiplex network. Using a supra-adjacency matrix representation of these systems we build on the communicability matrix and prove that the communicability function naturally induces an embedding of the multiplexes in a Euclidean space. We define in this way the communicability distances and angles between pairs of nodes in the multiplexes. These geometric parameters are split into: (i) intra-layer metrics, (ii) inter-layer metrics, and (iii) inter-layer self-metrics. In the first case, the pair of nodes under consideration are in the same layer of the multiplex. In the second case one node is in one layer and the other node in a different one. Finally, the inter-layer self-metrics account for the metrics between one node and itself in two different layers. Using these multiplex metrics we study two different multiplexes: a multiplex obtained as the result of 16 months of observation of politics on an office [33, 34] and a biological multiplex consisting of the synaptic interactions between 279 neurons in the worm *C. elegans* [35, 36]. We found that the average communicability angles in the multiplexes—which characterize the quality of communication between the nodes—change nonmonotonically with the coupling strength between the layers. Consequently, there is a value of the coupling strength for which such quality of communication is maximal, i.e. minimum average communicability angle. We provide an explanation for this phenomenon which emerges from the multiplexity of these systems and provide evidences for its implications, for instance in relation to the synchronizability of these systems. Finally, we define and study communicability shortest paths in the multiplexes. We show that they can be of two types: intra-layer paths, and multi-layer paths. In all cases we show how the communicability shortest paths avoid the most central nodes in the multiplexes in terms of their degree and betweenness. We found a theoretical justification for this behavior in terms of a diffusive model in which the 'information' not only diffuses between the nodes but it is also processed internally on the entities of the complex

system. Finally, we advance some ideas on how to extend the current work to account for other types of representation of complex systems, such as multiplex hypergraphs and multi-simplicial complexes.

2. Preliminaries

Here we start by defining formally what is a multiplex. A multiplex is the triple $\mathcal{M} = (G, \mathcal{A}, S)$, where $\mathcal{G} = \{G_1, \cdots, G_h\}$ is a set of simple graphs, in which $G_i = (V_i, E_i)$ where $V_i = \{v_1(i), \cdots, v_n(i)\}$ is a set of nodes and $E_i = \{(v_p(i), v_q(i))\}$ is a set of edges, $\mathcal{A} = \{\mathcal{A}(v_1), \cdots, \mathcal{A}(v_n)\}$ is a set of node identities, such that the following equivalence relation exists: $v_p(1) \overset{\mathcal{A}}{\equiv} v_p(2) \overset{\mathcal{A}}{\equiv} \cdots \overset{\mathcal{A}}{\equiv} v_p(h)$ for every node $v_p(i)$. Finally, $S = \{S_{1,2}, \cdots, S_{h-1,h}\}$, where $S_{ij} = \{\omega_1^{i,j}, \cdots, \omega_n^{i,j}\}$. The term $\omega_p^{i,j} = \omega(v_p(i), v_p(j))$ represents a weight (later known as coupling strength) for the pair $v_p \in V_i, v_p \in V_j$ for $i \neq j$. For instance, let $V_1 = \{a, b, c, d, e\}$, $V_2 = \{a', b', c', d', e'\}$, $E_1 = \{\{a, b\}, \{b, c\}, \{b, d\}, (c, d), \{d, e\}\}$, $E_2 = \{\{a', b'\}, \{b', c'\}, \{a', c'\}, \{b', c'\}, \{c', d'\}\}$, $\mathcal{A} = \{\text{Charles, Joan, Peter, Clare, Ann}\}$, such that $a \overset{\mathcal{A}}{\equiv} a'$, $b \overset{\mathcal{A}}{\equiv} b'$, $c \overset{\mathcal{A}}{\equiv} c'$, $d \overset{\mathcal{A}}{\equiv} d'$, $e \overset{\mathcal{A}}{\equiv} e'$, meaning for instance that the nodes a and a' both represent Charles, possibly in two different situations, e.g. using face-to-face contacts a, and communicating via Twitter a'. Let $S = \{\omega\{i, i'\}\}$, where $i = \{a, b, c, d, e\}$ then the multiplex corresponds to the one illustrated in figure 1(b). Here after we will call every graph G_i in the multiplex a layer, e.g. the layer L_i, and the weights ω the interlayer coupling strength.

A way to represent the topology of the multiplex $\mathcal{M}$ is by means of the supra-adjacency matrix $\mathscr{A}$, which is defined by

$$\mathscr{A} = \mathcal{A}_L + C_{LL}, \tag{2.1}$$

where

$$\mathcal{A}_L = \oplus_{\alpha=1}^{h} \mathcal{A}_\alpha = \begin{pmatrix} \mathcal{A}_1 & 0 & \cdots & 0 \\ 0 & \mathcal{A}_2 & \cdots & 0 \\ \vdots & \vdots & \ddots & \vdots \\ 0 & 0 & \cdots & \mathcal{A}_h \end{pmatrix}, \tag{2.2}$$

and

$$C_{LL} = \begin{pmatrix} 0 & C_{12} & \cdots & C_{1h} \\ C_{21} & 0 & \cdots & C_{2h} \\ \vdots & \vdots & \ddots & \vdots \\ C_{h1} & C_{h2} & \cdots & 0 \end{pmatrix}. \tag{2.3}$$

Here, the matrices A_i are the adjacency matrices of the individual layers of the multiplex and C_{ij} represents the connection of the nodes in the layer L_i with themselves in the layer L_i. If we consider that $C_{ij} = C$ for all the pairs of layers in the multiplex we can write

$$C_{LL} = C \otimes (O - I), \tag{2.4}$$

where $C = \omega I$ in which ω is the strength coupling between the layers, O is an all-ones matrix and I is the identity matrix.

Let us now define a multiplex walk. First, let us remind that a walk $v_0 \rightarrow v_m$ on a graph $G = (V, E)$ is an arbitrary sequence of nodes and edges $v_0, e_1, v_1, \ldots, e_m, v_m$ where each e_i is an (v_{i-1}, v_i) edge. The length of this walk $W_m(G)$ is the number m of its edges (including repeated edges).

Let us define a *jump* $J_k(i, j)$ between layers i and j as the sequence $v_p(i)\omega_p^{i,j}v_p(j)\omega_p^{j,i} \ldots \omega_p^{i,j}v_p(j)$ where the length of the sequence is the number of times the interlayer edges $\omega_p^{i,j}$ and $\omega_p^{j,i}$ are repeated. For instance, $J_1(i, j) = v_p(i)\omega_p^{i,j}v_p(j)$ and $J_3(i, j) = v_p(i)\omega_p^{i,j}v_p(j)\omega_p^{j,i}v_p(i)\omega_p^{i,j}v_p(j)$. Then, a *multiplex walk* is either a walk in a single layer $W_m(G_i)$ or a concatenation:

$$W_{m_1}(G_i)\|J_{m_2}(i, j)\|W_{m_3}(G_j) \cdots W_{m_{l-2}}(G_s)\|J_{m_{l-1}}(s, t)\|W_{m_l}(G_s),$$

where the length of the multiplex walk is $m_1 + \cdots + m_l$. A *closed multiplex walk* is a multiplex walk for which the initial and final nodes are the same. Notice that in counting the number of walks we consider the weight of the inter-layer connection. Then the weight of $J_k(i, j)$ is the product of the weights of all k inter-layer edges in this jump. A *multiplex path* is a multiplex walk with no repeated nodes. These paths can be weighted or not depending on whether we consider or not the weights of the inter-layer edges, respectively. Here we always consider unweighted paths.

It is easy to prove that $(\mathscr{A}^k)_{pq}$ counts the number of multiplex walks of length k between the nodes p and q in the multiplex. Similarly, $(\mathscr{A}^k)_{pp}$ counts the number of closed multiplex walks of length k that start at the node p. Then, we can account for all the multiplex walks of every length between every pair of nodes by considering the

following Taylor series:

$$\mathcal{G} = I + \mathcal{A} + \frac{\mathcal{A}^2}{2!} + \cdots = \sum_{k=0}^{\infty} \frac{\mathcal{A}^k}{k!} = \exp(\mathcal{A}), \tag{2.5}$$

where we have penalized the walks according to their length. That is, a multiplex walk of length s is penalized by $\frac{1}{s!}$. The nondiagonal entries of this exponential matrix are known as the communicability function between the corresponding pair of nodes [37–39]. The function $\mathcal{G}_{uv}$ counts the total number of walks starting at node u and ending at node v, weighted in decreasing order of their length by a factor $\frac{1}{k!}$. That is, the communicability function considers shorter walks more influential than longer ones and penalize them appropriately such that the whole series converges. The G_{uu} terms of the communicability function characterize the degree of participation of a node in all subgraphs of the network, giving more weight to the smaller ones. Thus, it is known as the subgraph centrality of the corresponding node [40].

The communicability matrix of a multiplex has the following block structure [41]:

$$\mathcal{G} = \exp(\mathcal{A}) = \begin{pmatrix} \mathcal{G}_{L_1} & \mathcal{G}_{L_1L_2} & \cdots & \mathcal{G}_{L_1L_h} \\ \mathcal{G}_{L_2L_1} & \mathcal{G}_{L_2} & \cdots & \mathcal{G}_{L_2L_h} \\ \vdots & \vdots & \ddots & \vdots \\ \mathcal{G}_{L_hL_1} & \mathcal{G}_{L_hL_2} & \cdots & \mathcal{G}_{L_h} \end{pmatrix}, \tag{2.6}$$

where the blocks $\mathcal{G}_{L_i}$ represent the communicability between pairs of nodes in the same layer L_i and $\mathcal{G}_{L_iL_j}$ accounts for the communicability between a node in the layer L_i and another in the layer L_j. Obviously, if the coupling between every pair of layers is exactly equal to zero we have that

$$\mathcal{G} = \begin{pmatrix} \exp(\mathcal{A}_1) & 0 & \cdots & 0 \\ 0 & \exp(\mathcal{A}_2) & \cdots & 0 \\ \vdots & \vdots & \ddots & \vdots \\ 0 & 0 & \cdots & \exp(\mathcal{A}_h) \end{pmatrix}. \tag{2.7}$$

3. Hyperspherical embedding of multiplexes

Hereafter we consider that the coupling strength between the layers in the multiplex is always the same between every pair of layers and that it is always positive. We label the eigenvalues of $\mathcal{A}$ in non-increasing order: $\lambda_1 \geqslant \lambda_2 \geqslant \ldots \geqslant \lambda_n$. Since $\mathcal{A}$ is a real-valued, symmetric matrix, we can decompose $\mathcal{A}$ into $\mathcal{A} = U\Lambda U^T$, where Λ is a diagonal matrix containing the eigenvalues of $\mathcal{A}$ and $U = [\overrightarrow{\psi}_1,\ldots,\overrightarrow{\psi}_n]$ is orthogonal, where $\overrightarrow{\psi}_i$ is an eigenvector associated with λ_i. Because the graphs considered here are connected, $\mathcal{A}$ is irreducible and from the Perron-Frobenius theorem we can deduce that $\lambda_1 > \lambda_2$ and that the leading eigenvector $\overrightarrow{\psi}_1$, which will be sometimes referred to as the Perron vector, can be chosen such that its components $\psi_1(u)$ are positive for all $u \in V$. A row of the matrix U corresponding to the node i of the graph is designated here by the vector $\vec{\varphi}_i = [\psi_1(i),\ldots\psi_n(i)]^T$.

Because $\mathcal{G} = \exp(\mathcal{A})$ is a positive definite matrix we can express it as a Gram matrix of the form

$$\mathcal{G} = \mathcal{X}^T\mathcal{X}, \tag{3.1}$$

where $\mathcal{X} = [\vec{x}_1,\ldots,\vec{x}_n]$ and

$$\vec{x}_u = \exp(\Lambda/2)\,\vec{\varphi}_u, \tag{3.2}$$

Then we can show that

$$\begin{aligned} \vec{x}_u \cdot \vec{x}_v &= (\exp(\Lambda/2)\,\vec{\varphi}_u)^T \exp(\Lambda/2)\,\vec{\varphi}_v \\ &= \vec{\varphi}_u^T \exp(\Lambda/2)\exp(\Lambda/2)\,\vec{\varphi}_v \\ &= \vec{\varphi}_u^T \exp(\Lambda)\,\vec{\varphi}_v \\ &= \sum_{j=1}^{n} e^{\lambda_j}\psi_j(u)\psi_j(v) \\ &= \mathcal{G}_{uv}. \end{aligned} \tag{3.3}$$

Our main goal now is to define a metric for the multiplex that accounts for the difference between the number of weighted closed walks that start at (and return to) the corresponding node u (respectively v), and the number of weighted walks that start at node u (respectively v) and ends at the node v (respectively u). This difference, which is defined below as ξ^2_{uv} serves as a quantification of the quality of communication channels

between two nodes. That is, if there are many routes that connect nodes u and v together, and there are not many routes that starting at the node u (respectively v) return to it, we can say that most of 'information' departing the node u (respectively v) with destination to the node v (respectively u) will arrive at its destination. Thus, there is a good quality of communication between these two nodes. The other way around is very clear as if there are many returning routes to the nodes and very few connecting them, most of the information departing one node will hardly arrive at the other. Let us now define these terms formally. Based on the previous intuition we define the following quantity:

$$\xi_{uv}^2 = \mathcal{G}_{uu} + \mathcal{G}_{vv} - 2\mathcal{G}_{uv}. \tag{3.4}$$

Another way of expressing this 'quality of communication' is by considering the ratio of these terms instead of their difference. That is

$$\gamma_{uv} = \frac{\mathcal{G}_{uv}}{\sqrt{\mathcal{G}_{uu}\mathcal{G}_{vv}}}. \tag{3.5}$$

We can easily show that

$$\begin{aligned}\xi_{uv}^2 &= \vec{x}_u \cdot \vec{x}_u + \vec{x}_v \cdot \vec{x}_v - 2\vec{x}_u \cdot \vec{x}_v \\ &= \|\vec{x}_u - \vec{x}_v\|^2.\end{aligned} \tag{3.6}$$

This expression clearly means that ξ_{uv}^2 is a Euclidean distance (metric) between the corresponding nodes in the multiplex. Previously we have proved that the Euclidean space in which this distance is defined for a pair of nodes in any network [42, 43] is an n-dimensional sphere [44]. That is, the communicability distance ξ_{uv}^2 induces an embedding of the multiplex $\mathcal{M}$ of size n into an $(n-1)$-sphere, of radius $R^2 = \frac{1}{4}\left(c - \frac{(2-b)^2}{a}\right)$, where $a = \vec{1}^T \exp(-\mathcal{A})\,\vec{1}$, $b = \vec{s}^T \exp(-\mathcal{A})\,\vec{1}$, $c = \vec{s}^T \exp(-\mathcal{A})\vec{s}$, and $\vec{s} = \mathrm{diag}(\exp(\mathcal{A}))$, and $\vec{s} = \mathrm{diag}(\mathcal{G})$.

On the other hand, it is straightforward to realize that

$$\theta_{uv} = \cos^{-1}\gamma_{uv} = \cos^{-1}\frac{\vec{x}_u \cdot \vec{x}_v}{\|\vec{x}_u\|\,\|\vec{x}_v\|}, \tag{3.7}$$

which means that θ_{uv} is the angle between the position vectors of the nodes u and v in the multiplex embedded in the $(n-1)$-sphere.

We can now construct two matrices that tabulate all the pairs of communicability distances and angles between all the pairs of nodes in a multiplex. Let us call these matrices $D(\mathcal{M})$ and $Z(\mathcal{M})$, respectively. Let us build the following vector: $\vec{s} = \mathrm{diag}(\mathcal{G})$, which is the main diagonal of the communicability matrix of the multiplex. Then, we can write these matrices as

$$D = D(\mathcal{M}) = (\vec{s}\cdot\vec{1}^T + \vec{1}\cdot\vec{s}^T - 2\mathcal{G})^{\odot(1/2)}, \tag{3.8}$$

$$Z = Z(\mathcal{M}) = \cos^{-1}\{\mathcal{G} \oslash [(\vec{s}\cdot\vec{1}) \odot (\vec{1}\cdot\vec{s})]\}^{\odot(1/2)}, \tag{3.9}$$

where $\oslash$ stands for the entrywise division, $\odot$ for the Hadamard product (entrywise product) of two matrices or entrywise power of a given matrix, and $\cdot$ for the inner product of two vectors. Here, $\vec{s} = \mathrm{diag}(\mathcal{G})$, $\mathcal{G} = \exp(\mathcal{A})$ and $\vec{1}$ is an all-ones vector.

We can write this communicability distance matrix in terms of the different block matrices that conform it, such that

$$D^{\circ 2} = \begin{pmatrix} S_{L_1} & S_{L_1} & \cdots & S_{L_1} \\ S_{L_2} & S_{L_2} & \cdots & S_{L_2} \\ \vdots & \vdots & \ddots & \vdots \\ S_{L_h} & S_{L_h} & \cdots & S_{L_h} \end{pmatrix} + \begin{pmatrix} S_{L_1} & S_{L_2} & \cdots & S_{L_h} \\ S_{L_1} & S_{L_2} & \cdots & S_{L_h} \\ \vdots & \vdots & \ddots & \vdots \\ S_{L_1} & S_{L_2} & \cdots & S_{L_h} \end{pmatrix} - 2\begin{pmatrix} \mathcal{G}_{L_1} & \mathcal{G}_{L_1L_2} & \cdots & \mathcal{G}_{L_1L_h} \\ \mathcal{G}_{L_2L_1} & \mathcal{G}_{L_2} & \cdots & \mathcal{G}_{L_2L_h} \\ \vdots & \vdots & \ddots & \vdots \\ \mathcal{G}_{L_hL_1} & \mathcal{G}_{L_hL_2} & \cdots & \mathcal{G}_{L_h} \end{pmatrix}, \tag{3.10}$$

where $S_{L_i} = (\vec{s}_{L_i}, \cdots, \vec{s}_{L_i})$ is an $n \times n$ matrix and $\vec{s}_{L_i} = (\mathcal{G}_{L_i}(1,1), \mathcal{G}_{L_i}(2,\ 2), \cdots, \mathcal{G}_{L_i}(n,\ n))^T$. Then, obviously we have that the communicability distance matrix can be written as

$$D^{\circ 2} = \begin{pmatrix} D_{L_1} & D_{L_1L_2} & \cdots & D_{L_1L_h} \\ D_{L_2L_1} & D_{L_2} & \cdots & D_{L_2L_h} \\ \vdots & \vdots & \ddots & \vdots \\ D_{L_hL_1} & D_{L_hL_2} & \cdots & D_{L_h} \end{pmatrix}. \tag{3.11}$$

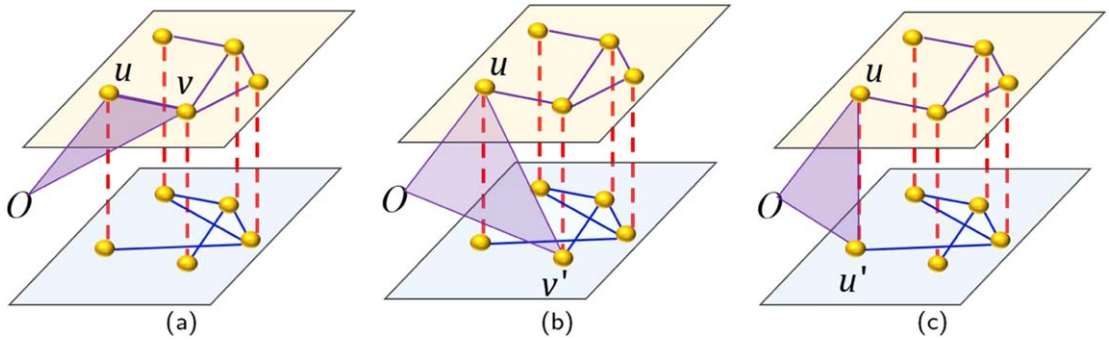

Figure 2. Different types of communicability distances and angles in a multiplex. (a) Intra-layer, $u \in L_i, v \in L_i$; (b) Inter-layer, $u \in L_i$, $v' \in L_j$; (c) Self-angle, $u \in L_i$, $u' \in L_j$. The triangles uOv, uOv', uOu', define the communicability distance as the length of the segments $\overline{uv}$, $\overline{uv'}$ and $\overline{uu'}$ as well as the communicability angles by $\angle uOv$, $\angle uOv'$, and $\angle uOu'$, respectively.

In a similar way we can express the communicability angles matrix as

$$Z^{\circ 2} = \begin{pmatrix} Z_{L_1} & Z_{L_1L_2} & \cdots & Z_{L_1L_h} \\ Z_{L_2L_1} & Z_{L_2} & \cdots & Z_{L_2L_h} \\ \vdots & \vdots & \ddots & \vdots \\ Z_{L_hL_1} & Z_{L_hL_2} & \cdots & Z_{L_h} \end{pmatrix}. \tag{3.12}$$

The individual entries of each of these two block matrices define the different communicability distances and angles given below:

- Intra-layer metrics

$$\xi^2_{L_i}(u \in L_i, v \in L_i) = \mathcal{G}_{L_i}(u, u) + \mathcal{G}_{L_i}(v, v) - 2\mathcal{G}_{L_i}(u, v), \tag{3.13}$$

$$\theta_{L_i}(u \in L_i, v \in L_i) = \cos^{-1}\frac{\mathcal{G}_{L_i}(u, v)}{\sqrt{\mathcal{G}_{L_i}(u, u)\mathcal{G}_{L_i}(v, v)}}. \tag{3.14}$$

- Inter-layer metrics

$$\xi^2_{L_iL_j}(u \in L_i, v' \in L_j) = \mathcal{G}_{L_i}(u, u) + \mathcal{G}_{L_j}(v', v') - 2\mathcal{G}_{L_iL_j}(u, v'), \tag{3.15}$$

$$\theta_{L_iL_j}(u \in L_i, v' \in L_j) = \cos^{-1}\frac{\mathcal{G}_{L_iL_j}(u, v')}{\sqrt{\mathcal{G}_{L_i}(u, u)\mathcal{G}_{L_j}(v', v')}}. \tag{3.16}$$

- Inter-layer self-metrics

$$\xi^2_{L_iL_j}(u \in L_i, u' \in L_j) = \mathcal{G}_{L_i}(u, u) + \mathcal{G}_{L_j}(u', u') - 2\mathcal{G}_{L_iL_j}(u, u'), \tag{3.17}$$

$$\theta_{L_iL_j}(u \in L_i, u' \in L_j) = \cos^{-1}\frac{\mathcal{G}_{L_iL_j}(u, u')}{\sqrt{\mathcal{G}_{L_i}(u, u)\mathcal{G}_{L_j}(u', u')}}. \tag{3.18}$$

In figure 2 we illustrate these geometric parameters for a simple multiplex.

4. Applications

Here we consider two multiplexes, one representing a social system and the other a biological one. The social system consists of a multiplex obtained as the result of 16 months of observation of an office politics [33]. The office is formed by 15 members of an overseas branch of a large international organization. This multiplex is formed by two layers, the first layer corresponds to the formal organizational chart of the employees, whereas the second layer represents the informal association among the employees. The biological multiplex consists on the synaptic interactions between 279 neurons in the worm *C. elegans* [35, 36]. The three layers of this multiplex

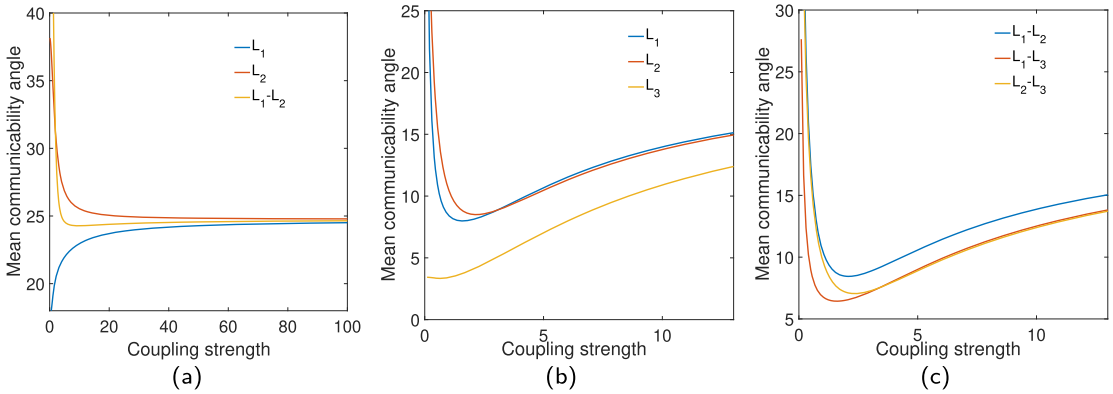

Figure 3. Plot of mean intra-layer communicability angles $\langle\theta_{L_i}\rangle$ versus interlayer coupling for the individual layers and average inter-layers communicability angle $L_i - L_j$ for the multiplexes representing Thurman office (a) and the *C. elegans* neuronal system (b) and (c).

represent different types of synaptic junctions: electric (el), chemical monadic (ch), and polyadic (pol) [35, 36]. A previous study has also considered multiplexes for the analysis of functional brain networks [45].

4.1. Communicability angles in multiplexes

The communicability angle averaged over all pairs of nodes $\langle\theta\rangle$ has been shown to represent a measure of 'communication efficiency' of graphs and networks [46]. This measure is bounded, in simple networks and multiplexes, as $0^\circ \leqslant \langle\theta\rangle \leqslant 90^\circ$, where the lower bound indicates a large average communication efficiency between pairs of nodes. This quantification of communication efficiency comes from the fact that the numerator of the communicability angle $\mathscr{G}_{pq}$ represents the capacity of two nodes to transfer 'information' between them. On the other hand, the denominator accounts for the amount of information that departs from a given node and returns to it after wandering around the network. That is, it is a sort of lost information as it is not properly delivered to its destination but returned to its originator. The fact that the communicability angles are always bounded allows us to compare it between different layers in the same multiplex as well as between different multiplexes.

In the figure 3 we plot the values of the mean communicability angles for the different layers of the two multiplexes studied, i.e. $\langle\theta_{L_i}\rangle$ as well as the average inter-layer angles, i.e. $\langle\theta_{L_iL_j}\rangle$, as a function of the inter-layer strength ω. In the corporate office (figure 3(a)) it is clear that the layer representing the formal communication between members L_1 displays more communication efficiency than the informal layer L_2 when the coupling strength is relatively small. When the coupling strength increases systematically the mean communicability angles of both layers tend to an equilibration point as a result of the decrease in efficiency on the formal layer and a gain in efficiency in the informal one. The inter-layer communicability angle decays very quickly with the increase of the inter-layer coupling and tends to the equilibration point determined by the two individual layers. The situation is similar for the case of the synaptic connections in the neural system of *C. elegans* where the layer representing polyadic synapses is more efficient than the layers of electric and of chemical synapses. However, here the layers of electrical and chemical synapses display a non-monotonic behavior with a minimum angle at around $\omega = 2$ (see further details). This non-monotonic behavior is also observed for the inter-layer angles as can be seen in figure 3(c), but here again a tendency to an equilibration between the three layers is observed. This equilibration of the mean communicability angles reflect the unique nature of the multiplex systems and it will be discussed with more details later. However, we would like to stress here that it represents a sort of averaging of the communication efficiency taking place in multiplexes, in which the isolated layers may display very different communication efficiencies, which are averaged in the aggregate network, i.e. when $\omega \to \infty$. However, the non-monotonic behavior of this efficiency may represent a unique characteristic of multiplexes that differentiate them qualitatively and quantitatively from both the isolated layers and the aggregate network.

We now consider the communicability angles averaged for all the layers on the multiplexes, i.e. the global intra-layer communicability angles, as a function of the inter-layer coupling strength. As can be seen in the figures 4(a) and (b) the global intra-layer communicability angles display a clear non-monotonic behavior. It dramatically drops to a minimum value, which is observed at $\omega \approx 8.8$ for the corporate office and at $\omega \approx 1.1$ for the neural multiplex of *C. elegans*. The situation is very similar if we consider instead the global average angles defined as the mean intra-, inter-layer and self angles. After these minima the communicability angles increase to an asymptotic value which depends on the multiplex analyzed. The reason why these minima exist is the following. Let us consider two layers L_i and L_j which are coupled with coupling strength ω. Let us assume that

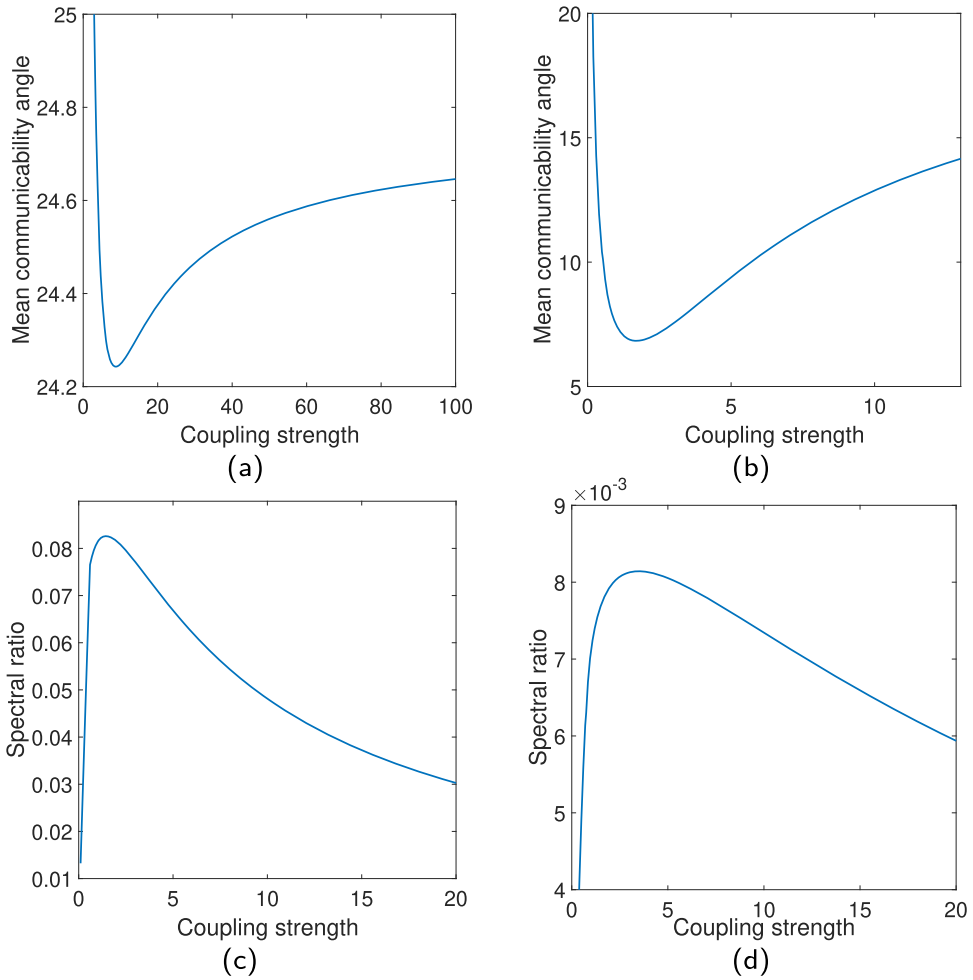

Figure 4. Plot of mean intra-layer communicability angles, i.e. mean for all the layers, (a) and (b), and the eigen ratios μ_2/μ_n (c) and (d) of the multiplexes representing the Thurman office (a), (c) and the *C. elegans* neuronal system (b), (d) as a function of the inter-layer coupling strength.

communication between the nodes is more efficient in one layer than in the other. For instance, let us consider that $\langle\theta_{L_i}\rangle > \langle\theta_{L_j}\rangle$. Then, as the coupling strength increases, the most efficient layer L_j starts to increase its average communicability angle as a consequence of the tendency of the multiplex of equilibrating the communication efficiency between both layers. On the other hand, the layer with the worse communication efficiency starts to improve it and as a consequence reduces its average communicability angle. The rate at which these layers tend to equilibrate their communication efficiency appears to follow (based on our empirical observations) an exponential law. That is, $\langle\theta_{L_i}(\omega)\rangle \sim \mathcal{A}\exp(-\alpha\omega)$ and $\langle\theta_{L_j}(\omega)\rangle \sim -B\exp(-\beta\omega)$. These equilibration rates result in the curves that we observed in figure 3. For instance, for the corporate office L_1 is the layer following $\langle\theta_{L_1}(\omega)\rangle \approx 23.73 - 5.721\exp(-0.211\omega)$ and L_2 follows $\langle\theta_{L_2}(\omega)\rangle \approx 24.89 + 14.44\exp(-0.399\omega)$. It is important to remark that the critical behavior, i.e. the existence of a critical value of the coupling strength for which the communicability angle is minimum, occurs only if $\alpha \neq \beta$. That is, if the rates at which one of the layers increases its efficiency and the other decreases it, are different. In this case the global intra-layer efficiency follows a law to equilibration of the form $\langle\theta_{L_i}(\omega) + \theta_{L_j}(\omega)\rangle \sim \mathcal{A}\exp(-\alpha\omega) - B\exp(-\beta\omega)$. In this case the critical coupling strength is

$$\omega_c = \frac{\ln\left(\frac{\mathcal{A}\alpha}{B\beta}\right)}{\alpha - \beta}. \tag{4.1}$$

This means that the location of the minimum depends only on the rate at which the corresponding layers equilibrate their communication efficiency expressed in terms of the communicability angles. With more layers the situation is more complicated for finding the location of the minimum but the meaning of it is exactly the same. In order to see the implications of this nonmonotonic change of the communicability angle with the coupling strength in multiplexes we have studied three other important spectral parameters of networks. They are the spectral radius of the supra-adjacency matrix $\mathscr{A}$, i.e. the largest eigenvalue $\lambda_1(\mathscr{A})$; the spectral gap

$\lambda_1(\mathscr{A}) - \lambda_2(\mathscr{A})$; the spectral eigenratio of the second smallest and the largest eigenvalues of the Laplacian matrix of the whole multiplex, $Q = \mu_2/\mu_n$. The first spectral parameter is very important for understanding spreading processes such as epidemic propagation on networks due to its relation to the epidemic spreading [47]. The second parameter is related to the good expansion properties of networks [48, 49]. That is, a large spectral gap implies that the network is super-homogeneous in the sense that 'what you see locally is what you get globally'. Finally, the eigenratio Q is related to the synchronizability of a connected network, with largest values of Q corresponding to the largest synchronizability of the corresponding network [50]. In the two multiplexes studied here neither $\lambda_1(\mathscr{A})$ nor $\lambda_1(\mathcal{A}) - \lambda_2(\mathcal{A})$ display any non-monotonic behavior with the change of ω. The spectral radius increases almost linearly with ω, while the spectral gap changes nonlinearly but monotonically with ω (plots not shown). However, the eigenratio Q displays a clear nonmonotonic behavior in both multiplexes. As can be seen in figures 4(c) and (d), Q has a maximum at $\omega = 1.5$ for the corporate office and at$\omega = 0.8$ for the neural system of *C. elegans*. In the case of the corporate office the minima observed for the communicability angle and for the eigenratio are relatively far from each other. However, the two minima in the neural system of *C. elegans* are very close to each other. The reason explaining why we observe this nonmonotonic behavior for the eigenratio is the following. The communicability angle changes with the variation in the homogeneity of the network. Understanding by homogeneity, not its degree distribution, but the absence of structural bottlenecks or more exactly the presence of 'good expansion properties', i.e. the existence of very few nodes and/or edges whose removal disconnect the network into two parts of approximately the same size [48, 49]. For instance, $\mathscr{G}_{uv}/\sqrt{\mathscr{G}_{uu}\mathscr{G}_{vv}} \rightarrow 1$ indicates that there are as many walks going from u to v as the sum of those returning to u and to v. If the average of these angles is then close to zero it indicates a great homogeneity in the network. However, if $\mathscr{G}_{uv}/\sqrt{\mathscr{G}_{uu}\mathscr{G}_{vv}} \rightarrow 0$ means that there are very few walks connecting the two nodes, thus removing some of the nodes/edges in these walks may disconnect the network. In closing, when the communicability angle is close to zero ($\mathscr{G}_{uv}/\sqrt{\mathscr{G}_{uu}\mathscr{G}_{vv}} \rightarrow 1$) for most pairs of nodes in the network, the network may display good expansion properties. It has been shown previously that such good expansion networks, a.k.a. entangled networks, display the best syncronizability, i.e. the highest values of the eigenratio Q [51]. Thus, as the communicability angle, i.e. the homogeneity of the network, change nonmonotonically with the coupling strength for the multiplexes studied (due to the reasons explained before), also the eigenratio changes in a similar fashion.

4.2. Shortest communicability paths in multiplexes

In this part of the work we study how information can travel in a multiplex if it were using the communicability paths instead of the (topological) shortest paths between nodes. Let us start by defining what we understand by the communicability shortest path between two nodes. Let us consider a multiplex $\mathcal{M}$ with supra-adjacency matrix $\mathscr{A}$ in which for every pair of connected nodes u and v, we assign the corresponding communicability distance ξ_{uv}. That is, we create a communicability-distance-weighted multiplex whose weighted supra-adjacency matrix is

$$W = \mathscr{A} \circ D = D \circ \mathscr{A}, \tag{4.2}$$

where D is the communicability distance matrix. Then, the shortest communicability path connecting two nodes in the multiplex $\mathcal{M}$ is the minimum weighted shortest path connecting both nodes in W. Here, the length of a weighted communicability path is the sum of the weights (communicability distances) of all the edges in the path. Notice that the (topological) shortest path between the corresponding two nodes is the minimum shortest path connecting both nodes in $\mathscr{A}$ instead of in W.

We now compare the communicability shortest paths with the (topological) shortest paths for some pairs of nodes in the corporate office studied by Thurman [33]. First, we select two pairs of individuals trying to communicate in the formal layer of the biplex. For instance, when Minna and Katy interchange information using the shortest path connecting them in the formal communication organization of the office they have to pass their information to Pete, who is the most central individual in the office. However, according to the communicability distance, it is 'shorter' for this information to arrive to its destination if Katty passes the information to Amy in the informal layer of communication, and Amy passes the information to Minna in the formal structure of the office. The representation of this shortest communicability path in the biplex is given in figure 5(a) when the coupling between the two layers is relatively small. Of course, in the real-life we cannot split ourselves into the 'formal' and the 'informal' layers of communication in an office. What this communicability shortest path between Amy and Minna indicates is the following. It is easier for Minna to chat informally with her friend Amy and give her certain information. Then, Amy can 'formally' communicate this information to Minna, who has then not received the information by the 'formal channel' established in the office for transmitting information, e.g. via Pete or the President. We can see the same situation for another pair of agents in the office: Minna and Emma. In this case, Minna and Emma are not connected in the formal layer but they are in the informal one. Thus, it is easier for them to share such information informally than communicating

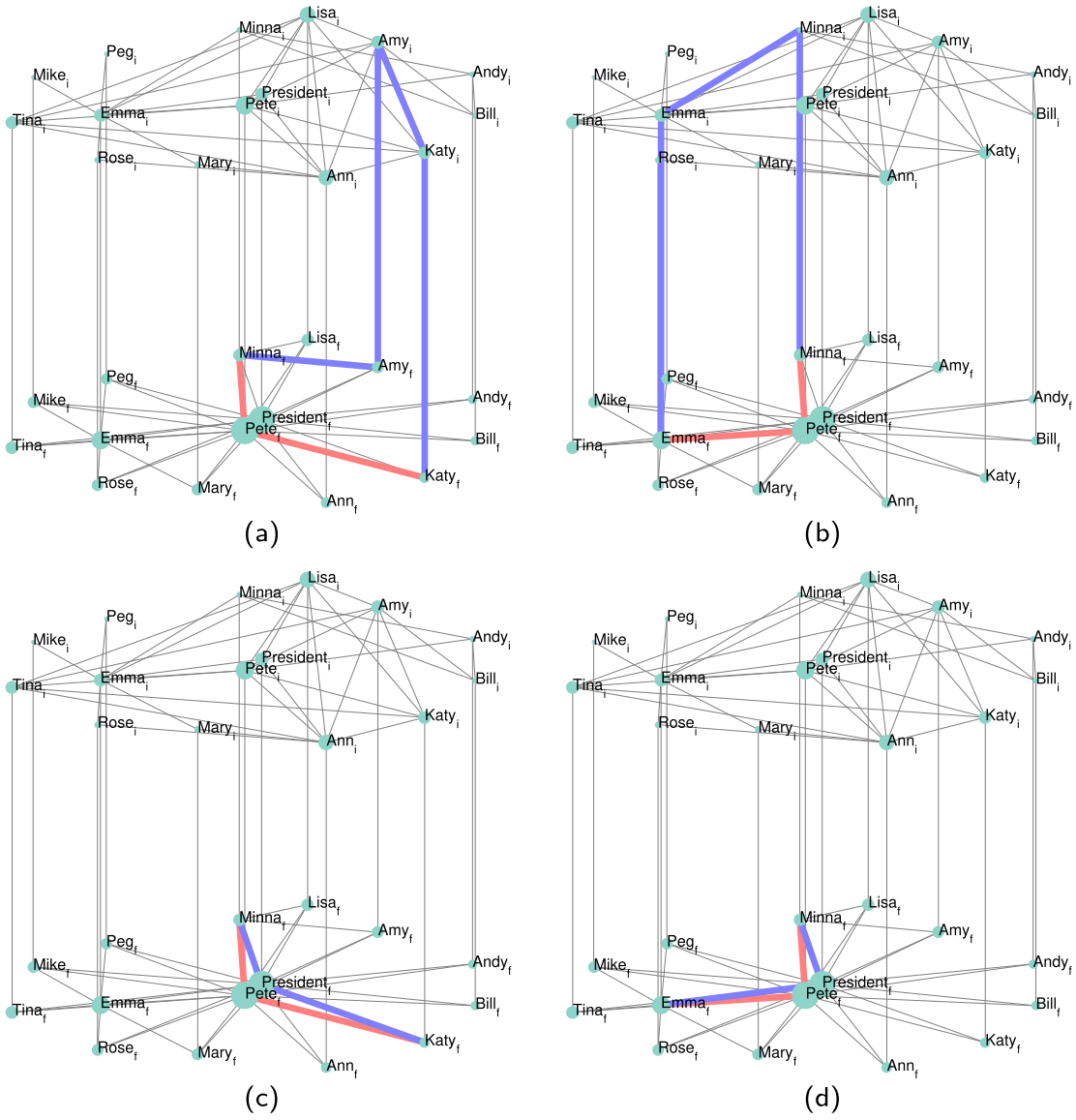

Figure 5. Shortest path (red segments) and shortest communicability path (blue segments) based on communicability distance between two pairs (Minna–Katy and Emma–Bill) of members of the office in the formal layer with weak coupling between layers, $\omega = 0.5$ (a) and (b), and with relatively large inter-layer coupling $\omega = 3.5$ (c) and (d).

through the formal channels existing in the office (see figure 5(b)). This 'distortion' of the formal routes of communication in an office can have important consequences for its well-functioning. It is known that in this overseas office of a corporation studied by Thurman [33] there was a conflict in which a coalition of attackers formed by Ann, Katy, Amy, Pete, Tina and Lisa attacked Minna and Emma. As reported by Thurman in his study [33]: '*Within the network a large number of rumors circulated rapidly among Pete, Ann, Amy, Katy, Tina, and Lisa.*' This is exactly what we observe with the use of the communicability shortest paths. The communication between members of the office and the two victims mainly takes place through the informal layer, which is mainly controlled by Ann, Katy, Amy, Pete, Tina and Lisa. Therefore, they have the chances of manipulating the information to affect the two victims. In figures 5(c) and (d) we observe that when the coupling strength between the two layers is sufficiently large the communication mainly take place through the shortest path. This means that in an aggregate network we are not able to 'see' the subtleties of the communication in this office that may explain some of its dynamics and problems taken place in it.

When the communication is intended solely at the informal level between two individuals, the shortest communicability path is maintained inside the informal layer as can be seen in figure 6. The main difference between these paths and the topological ones is that the first ones avoid the nodes with the largest centrality in the corresponding layer (see further analysis).

We now consider the multiplex representing the neural system of *C. elegans* which consists of three layers specifying the kind of synaptic interaction (electric, chemical or polyadic) between the neurons. Our goal here is

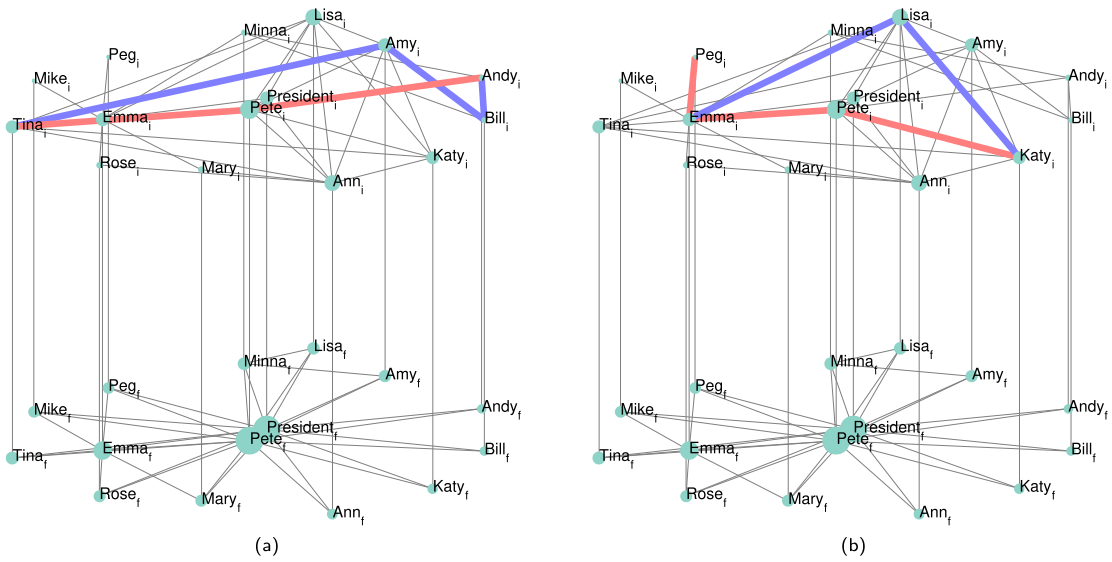

Figure 6. Shortest path (red segments) and shortest communicability paths (blue segments) based on communicability distance between two pairs (Tina–Andy and Peg–Katy) of members of the office in the informal layer with strong coupling between layers, $\omega = 3.5$.

not to give a detailed account of all the communicability shortest paths connecting different pairs of neurons. Instead we aim at stressing some of the main differences between the communicability shortest paths and the topological ones for a few pairs of neurons. First, we select a pair of neurons for which there is a shortest path formed by electric synapses only. It is the path $AIML_{el}$-$SIBDR_{el}$-$RIBR_{el}$-$SMDDR_{el}$-$VD01_{el}$. Instead, the communicability shortest path consists of a combination of electrical and chemical synapses: {$AIML_{el}$-$AIML_{ch}$}-$AIAL_{ch}$-$RMGL_{ch}$-$SAADR_{ch}$-$OLLL_{ch}$-{$SMDDR_{ch}$-$SMDDR_{el}$}-$VD01_{el}$. While the shortest topological path involves five different neurons, the shortest communicability one involves seven. Notice that we grouped in curly brackets those neurons which are essentially the same but having two different types of synapses. The main difference between these two paths is the centrality of the neurons involved in them. For instance, while the shortest topological path involves neurons with degrees: 3-5-**19**-6-10, the neurons in the shortest communicability have degrees: 3-6-**13**-10-11-9-9-6-10, where the highest degree is always given in bold.

We proceed with a topological shortest path connecting two neurons in which all synapses are of chemical nature: $AIAL_{ch}$-$ADLL_{ch}$-$AVBL_{ch}$-$PVCR_{ch}$. The alternative shortest communicability path involves again a combination of electrical and chemical synapses: $AIAL_{ch}$-$HSNL_{ch}$-{$AVJL_{ch}$-$AVJL_{el}$}-{$PVCR_{el}$-$PVCR_{ch}$}. Here both paths involve exactly the same number of neurons. However, the shortest topological path involves a very central neuron, which has degree 33, while the shortest communicability one does not involve any neuron with degree larger than 13. The two degree sequences are: 13-8-**33**-30 for the topological shortest path and 13-10-10-8-**13**-30 for the communicability one.

Finally, we illustrate the differences between the topological shortest path: $ADAR_{pol}$-$AVBL_{pol}$-$VC04_{pol}$, which involves only three neurons all with polyadic synapses and the shortest communicability path: {$ADAR_{pol}$-$ADAR_{el}$}-$ASHR_{el}$-{$RICR_{el}$-$RICR_{ch}$}-$URBL_{ch}$-$VC05_{ch}$-{$VC04_{ch}$-$VC04_{pol}$}, which involves 6 neurons and the three layers of the multiplex. In the shortest topological path there is a neuron with very high degree: 20-**41**-5, while in the communicability one all intermediate neurons are of low degree: 20-7-8-4-8-7-**11**-7-5. In figure 7 we illustrate the three pairs of paths mentioned before.

The differences in the centralities of the nodes in each type of path are more significant if we consider the betweenness centrality. In this case for the shortest path $AIML_{el} \rightarrow VD01_{el}$ the betweenness of intermediary neurons are: 393.3-**5 088.3**-563.2, while for the shortest communicability path they are: 471.4-**1 721.1**-1 501.0-1 365.9-643.1-683.7-563.2. That is, the neuron $RIBR_{el}$, which is in the shortest topological path, has almost three times more betweenness than the most central neuron in the communicability path, $AIAL_{ch}$. In the shortest path connecting $AIAL_{ch} \rightarrow PVCR_{ch}$ the betweenness of the intermediate neurons are: 782.3-**9 437.4**, while for the shortest communicability path they are: 2 119.2-981.1-582.6-**2 308.2**. That is, the most central neuron in the shortest path, $AVBL_{ch}$, has four times more betweenness than the most central one in the communicability path, $AVBL_{ch}$. Finally, in the path $ADAR_{pol} \rightarrow VC04_{pol}$ we have for the shortest path that the only intermediate neuron has betweenness equal to **7 569.3**, while for the communicability path we have: 395.2-618.1-239.4-

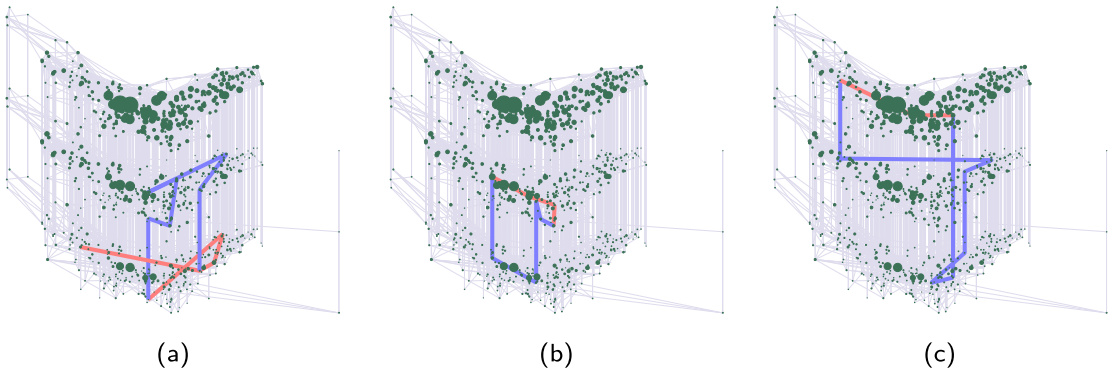

Figure 7. Shortest path (red segments) and shortest communicability paths (blue segments) based on communicability distance between three pairs of neurons in the *C. elegans* neuronal system. Every pair of neurons are located in the same layer: electronic (a), chemical (b) and polyadic (c). The interlayer coupling is $\omega = 0.5$ in all cases.

768.6-1 011.2-**1 955.2**-582.5. This means that the most central neuron in the shortest path, $AVBL_{pol}$, is almost four times more central than the most central one in the communicability path, $VC05_{ch}$.

Finally, if we consider the subgraph centrality of the nodes in each of the paths we observe that the most central neuron ($RIBR_{el}$) in the shortest path $AIML_{el} \rightarrow VD01_{el}$ is 1.7 times more central than that in the shortest communicability path ($RMGL_{ch}$). In the path $AIAL_{ch} \rightarrow PVCR_{ch}$ the most central neuron ($AVBL_{ch}$) in the shortest path is 3.6 times more central than the most central in the communicability path ($PVCR_{el}$). In the path $ADAR_{pol} \rightarrow VC04_{pol}$ the most central neuron in the shortest path ($AVBL_{pol}$) is 5600 times more central than the most central one in the communicability path ($ADAR_{el}$).

The clear conclusion from the last experiments concerning the centrality of the nodes in the shortest communicability paths in comparison with those in the shortest topological paths is the following. The nodes in the shortest communicability paths are significantly less central than the nodes in the shortest topological paths. In other words, the shortest communicability paths avoid to trespass the hubs of the network, understanding by hubs the most central nodes not only in terms of their degrees. A plausible explanation for this behavior is given in the next subsection of this work.

4.3. Diffusive communicability paths

In a diffusive process on a multiplex, the variation of the concentration in time $\vec{c}\,(t)$ is determined by the diffusion equation

$$\frac{\partial \vec{c}\,(t)}{\partial t} = -\mathcal{L}\vec{c}\,(t), \tag{4.3}$$

with the initial condition $\vec{c}\,(0) = \vec{c}_0$. In the previous equation $\mathcal{L}$ is the multiplex Laplacian, obtained from a diagonal matrix of nodes degrees $\triangle$ and the supra-adjacency matrix $\mathscr{A}$, i.e. $\mathcal{L} = \triangle - \mathscr{A}$, and we have set the diffusion coefficient to one. The degree of a node i is taken here as the number of connections the node i has in its corresponding layer of the multiplex plus the sum of the coupling strengths of this node to itself in all the other layers of the multiplex. The solution of (4.3) is given by $\vec{c}\,(t) = \exp(-t\mathcal{L})\vec{c}_0 = \exp(-t\triangle + t\mathscr{A})\vec{c}_0$. What this equation is telling us about the physical process taking place on the multiplex? This equation is describing a process in which the particles diffusing between the nodes of the multiplex take time only to 'decide' to which nearest neighbor node they will hop in the next time step. That is, the probability that the particle hops from node u in layer i to node v in the same layer (marked with magenta arrows in figure 8(a)) is $p_{L_iL_i}(u, v) = \frac{1}{k_u + \omega}$, where k_u is the number of connections of the node u in the layer i and ω is as before. On the other hand, the probability that the particle hops from node u in layer i to node u in the layer j (marked with a red arrow in figure 8(a)) is $p_{L_iL_j}(u, u) = \frac{\omega}{k_u + \omega}$. Obviously, $p_{L_iL_j}(u, v) = 0$ for $i \neq j$ and $u \neq v$. These probabilities, as well as equation (4.3), indicate that the diffusive particle does not take any time 'inside the nodes'. That is, the diffusive particle enters the node and abandon it as soon as it 'decides' to which other node to hop. This is of course a very unrealistic situation, which means that the nodes do not process information once it enters into them. In this model, nodes are there for nothing!

Let us consider now a more realistic situation in which every node 'processes' the diffusive particle entering into it. That is, the diffusive particle enters the node and spend some time in it as a consequence of certain chemical, biological or any other kind of processing. In general, this generates a 'waiting time' as known in the case of random walkers studies. For the sake of simplicity let us consider that such internal process is represented by a 'self-coupling' of a node to itself, which is translated in the network-theoretic language by a weighted self-

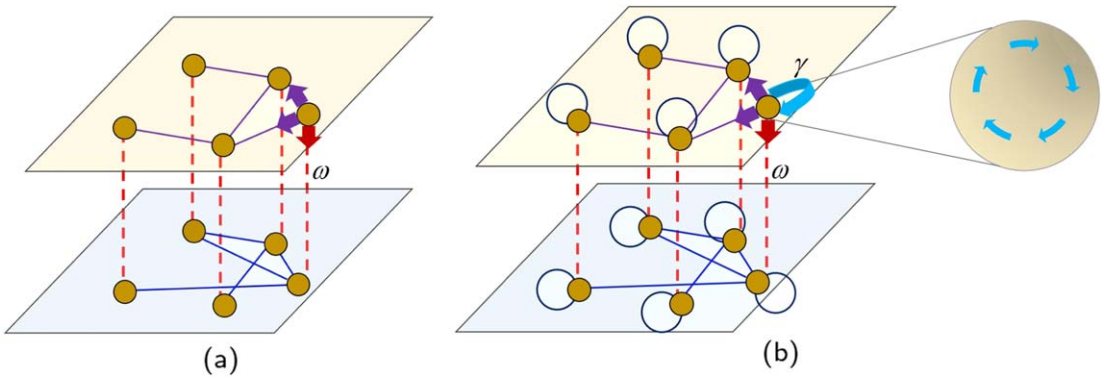

Figure 8. Illustration of the diffusion process in a multiplex where the information is not processed at the nodes (a) and when the information is processed at them (b). The processing of information is represented here by a weighted self-loop over each of the nodes. Here all the self-loop weights are the same but it is not necessarily always the case. The magenta arrows represent the ways of going out from a node in a given layer to another node in the same layer. The red arrow represent the way of moving from one node to itself in a different layer (see text for explanations).

loop (see figure 8(b)). This diffusive process is controlled by

$$\frac{\partial \vec{c}\,(t)}{\partial t} = -(\gamma I + \triangle - \mathscr{A})\vec{c}\,(t), \tag{4.4}$$

where I is the corresponding identity matrix and γ is the self-coupling of a node with itself. The self-coupling of a node with itself is a sort of resistance of the node to give the diffusive particle to a nearest neighbor. Let us assume that $\gamma = \alpha k_{\max}$ with $\alpha \gg 1$ for all nodes u in the multiplex, where $k_{\max}$ is the maximum degree of a node in the multiplex. That is, we are assuming that the processing of information inside a node is a process that requires significantly more time than the selection of the node to which such information will hop in the next time step. Now, we can write the diffusion equation of the whole multiplex as

$$\frac{\partial \vec{c}\,(t)}{\partial t} = -(\gamma I - \mathscr{A})\vec{c}\,(t). \tag{4.5}$$

After the previous transformation, the solution of the diffusion equation is given by

$$\begin{aligned}\vec{c}\,(t) &= (\exp(-t(\gamma I - \mathscr{A})))\vec{c}_0,\\ &= \exp(-t\gamma I)\exp(t\mathscr{A})\vec{c}_0,\\ &= \alpha(\gamma,\, t)\exp(t\mathscr{A})\vec{c}_0,\end{aligned} \tag{4.6}$$

where $\alpha(t,\, \gamma)$ is a constant for a given t and γ. For $t = 1$ we obviously have that $\vec{c}\,(t = 1) \sim \mathscr{G}\vec{c}_0$, where $\mathscr{G}$ is the communicability matrix. Thus, the shortest communicability paths found previously in this work represent the 'diffusion paths' for diffusive particles that not only hop between the nodes of the multiplex but also are 'processed' inside the nodes.

5. Future outlook

The communicability function of networks has found a plethora of interesting and useful applications in a large variety of fields. The geometry emerging from this communicability function has also started to find applications in different areas. These concepts have been extended beyond networks [42–44, 46] to account for information diffusion processes also in simplicial complexes [17]. Here we have extended the notion of communicability geometry to multiplexes. We have shown that this topological representation of complex systems in which nodes are sliced in different layers also 'lives' in a communicability Euclidean hyperspherical space. We have also advanced a formal definition of a simple multiplex as the triple $\mathcal{M} = (\mathcal{G},\, \mathcal{A},\, S)$, where $\mathcal{G}$ is a set of simple graphs, $\mathcal{A}$ is the set of node identities and S a set of interlayer weighted connections of the nodes. It is straightforward to realize that directed and weighted multiplexes are easily realizable from this definition by changing the set of simple graphs $\mathcal{G}$ by a set of directed and weighted graphs $\mathcal{G}'$. However, this representation allow also the extension of multiplexity to hypergraphs and simplicial complexes.

That is, if we define $\mathcal{H}$ as a set of hypergraphs instead of a set of simple graphs, then $\mathscr{M} = (\mathcal{H},\, \mathcal{A},\, S)$ represents a multiplex hypernetwork as illustrated in figure 9(a). In a similar way, if $\mathcal{K}$ is a set of simplicial complexes instead of a set of simple graphs, then $\mathfrak{M} = (\mathcal{K},\, \mathcal{A},\, S)$ is a multi-simplicial complex as the one illustrated in figure 9(b). Future efforts should be made to study these types of representation of complex

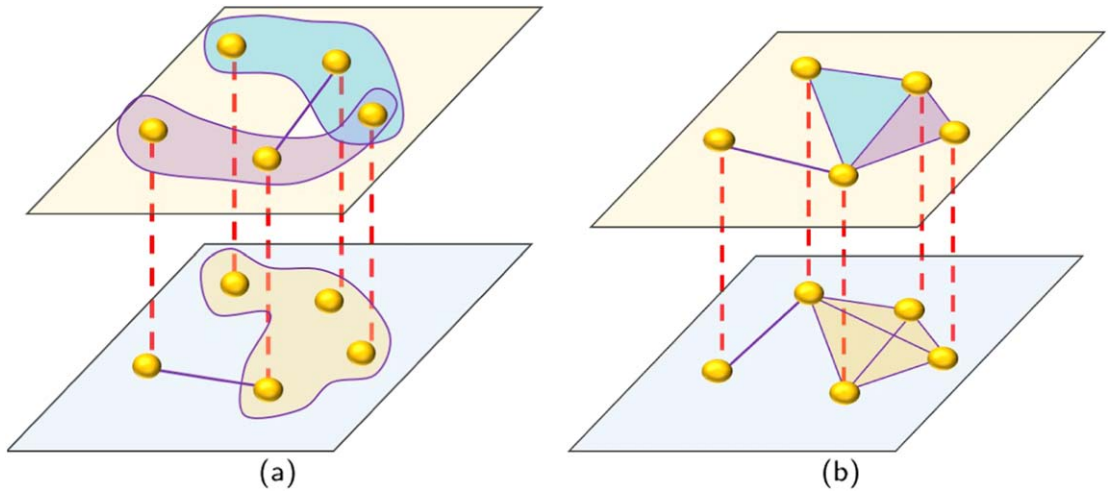

Figure 9. New types of representation of complex systems in the form of multiplex hypergraph (a) and multi-simplicial complex (b).

systems, their communicability function and geometry to see whether they bring new insights about the functioning of the systems they represent. We hope the current work open such new doors for the study of these systems.

ORCID iDs

Ernesto Estrada https://orcid.org/0000-0002-3066-7418

References

[1] Estrada E 2012 *The Structure of Complex Networks: Theory and Applications* (Oxford: Oxford University Press)
[2] Latora V, Nicosia V and Russo G 2017 *Complex Networks: Principles, Methods and Applications* (Cambridge: Cambridge University Press)
[3] Newman M E 2003 *SIAM Rev.* **45** 167–256
[4] Boccaletti S, Latora V, Moreno Y, Chavez M and Hwang D U 2006 *Phys. Rep.* **424** 175–308
[5] Barrat A, Barthelemy M and Vespignani A 2007 *Large Scale Structure And Dynamics Of Complex Networks: From Information Technology to Finance and Natural Science* (Singapore: World Scientific) pp 67–92
[6] Newman M E 2004 *Phys. Rev.* E **70** 056131
[7] Estrada E and Rodríguez-Velázquez J A 2006 *Physica* A **364** 581–94
[8] Sonntag M and Teichert H M 2004 *Discrete Appl. Math.* **143** 324–9
[9] Zlatić V, Ghoshal G and Caldarelli G 2009 *Phys. Rev.* E **80** 036118
[10] Gallo G, Longo G, Pallottino S and Nguyen S 1993 *Discrete Appl. Math.* **42** 177–201
[11] Klamt S, Haus U U and Theis F 2009 *PLoS Comput. Biol.* **5** e1000385
[12] Maletić S and Rajković M 2012 *Eur. Phys. J. Spec. Top.* **212** 77–97
[13] Giusti C, Ghrist R and Bassett D S 2016 *J. Comput. Neurosci.* **41** 1–14
[14] Maletić S and Rajković M 2014 *Physica* A **397** 111–20
[15] Kee K F, Sparks L, Struppa D C, Mannucci M A and Damiano A 2016 *Health Commun.* **31** 385–99
[16] De Silva V and Ghrist R 2007 *Algebr. Geom. Topol.* **7** 339–58
[17] Estrada E and Ross G J 2018 *J. Theor. Biol.* **438** 46–60
[18] Gutin G, Jones M, Sheng B, Wahlström M and Yeo A 2017 *Discrete Appl. Math.* **217** 196–202
[19] Boccaletti S, Bianconi G, Criado R, Del Genio C I, Gómez-Gardeñes J, Romance M, Sendiña-Nadal I, Wang Z and Zanin M 2014 *Phys. Rep.* **544** 1–122
[20] Kivelä M, Arenas A, Barthelemy M, Gleeson J P, Moreno Y and Porter M A 2014 *J. Complex Netw.* **2** 203–71
[21] Battiston F, Nicosia V and Latora V 2014 *Phys. Rev.* E **89** 032804
[22] Mucha P J, Richardson T, Macon K, Porter M A and Onnela J-P 2010 *Science* **328** 876–8
[23] Solé-Ribalta A, De Domenico M, Kouvaris N E, Diaz-Guilera A, Gómez S and Arenas A 2013 *Phys. Rev.* E **88** 032807
[24] De Domenico M, Solé-Ribalta A, Cozzo E, Kivela M, Moreno Y, Porter M A, Gómez S and Arenas A 2013 *Phys. Rev.* X **3** 041022
[25] Gómez-Gardeñes J, Reinares I, Arenas A and Floría L M M 2012 *Sci. Rep.* **2** 320
[26] Baxter J B, Dorogovtsev S N, Goltsev A V and Mendes J F F 2012 *Phys. Rev. Lett.* **109** 248701
[27] Cozzo E, Arenas A and Moreno Y 2012 *Phys. Rev.* E **86** 036115
[28] Bianconi G 2013 *Phys. Rev.* E **87** 062806
[29] Gómez S, Díaz-Guilera A, Gómez-Gardeñes J, Pérez-Vicente C J P, Moreno Y and Arenas A 2013 *Phys. Rev. Lett.* **110** 028701
[30] Granell C, Gómez S and Arenas A 2013 *Phys. Rev. Lett.* **111** 128701
[31] De Domenico M, Sole A, Gómez S and Arenas A 2014 *Proc. Natl Acad. Sci. USA* **111** 8351–6
[32] Radicchi F and Arenas A 2013 *Nat. Phys.* **9** 717–20

[33] Thurman B 1979 *Soc. Netw.* **2** 47–63
[34] Batagelj V and Mrvar A 2006 Pajek datasets http://vlado.fmf.uni-lj.si/pub/networks/data/
[35] Chen B L, Hall D H and Chklovskii D B 2006 *Proc. Natl Acad. Sci USA* **103** 4723–8
[36] De Domenico M, Porter M A and Arenas A 2015 *J. Complex Netw.* **3** 159–76
[37] Estrada E and Hatano N 2008 *Phys. Rev.* E **77** 036111
[38] Estrada E and Higham D J 2010 *SIAM Rev.* **52** 96–714
[39] Estrada E, Hatano N and Benzi M 2012 *Phys. Rep.* **514** 89–119
[40] Estrada E and Rodríguez-Velázquez J A 2005 *Phys. Rev.* E **71** 056103
[41] Estrada E and Gómez-Gardeñes J 2014 *Phys. Rev.* E **89** 042819
[42] Estrada E 2012 *Linear Algebr. Appl.* **436** 4317–28
[43] Estrada E 2012 *Phys. Rev.* E **85** 066122
[44] Estrada E, Sánchez-Lirola M G and de la Peña J A 2014 *Discrete Appl. Math.* **176** 53–77
[45] De Domenico M, Sasai S and Arenas A 2016 *Front. Neurosci.* **10** 326
[46] Estrada E and Hatano N 2016 *SIAM Rev.* **58** 692–715
[47] Chakrabarti D, Wang Y, Wang C, Leskovec J and Faloutsos C 2008 *ACM Trans. Inf. Syst. Sect. (TISSEC)* **10** 1
[48] Estrada E 2006 *Europhys. Lett.* **73** 649
[49] Hoory S, Linial N and Wigderson A 2006 *Bull. Am. Math. Soc.* **43** 439–561
[50] Barahona M and Pecora L M 2002 *Phys. Rev. Lett.* **89** 054101
[51] Donetti L, Hurtado P I and Muñoz M A 2005 *Phys. Rev. Lett.* **95** 188701